KINETICS AND MECHANISM OF PYROLYSIS OF LARCH AZOTANNINS

OLGA YU. FETISOVA,[*] NADEZHDA M. MIKOVA,[*] NATALYA YU. VASILYEVA,[*,**] SVETLANA A. NOVIKOVA[*] and ALEKSANDR S. KAZACHENKO[*,**,***,****]

[*]*Institute of Chemistry and Chemical Technology SB RAS, Federal Research Center "Krasnoyarsk Scientific Center SB RAS", Krasnoyarsk, 660036 Russia*
[**]*Institute of Non-Ferrous Metals, Siberian Federal University, Svobodny Avenue, 79, Krasnoyarsk, 660041, Russia*
[***]*Krasnoyarsk State Medical University, Partizana Zheleznyaka St., Bldg. 1, Krasnoyarsk, 660022, Russia*
[****]*Reshetnev Siberian State University of Science and Technology, Institute of Chemical Technologies, Prospekt Mira 82, Krasnoyarsk, Russia*
✉ *Corresponding author: A. S. Kazachenko, leo_lion_leo@mail.ru*

Received June 15, 2025

N-modified compounds were obtained on the basis of previously isolated tannins from larch (T). The estimated composition of the compounds obtained was analyzed by FTIR spectroscopy and elemental analysis. The thermal degradation of larch tannin and its nitrated compounds, such as nitrile azotannin (ATN) and cationic azotannin (CAT), has been studied using thermogravimetry at three heating rates of 5, 10 and 20°/min. Thermal stability of N-modified tannins depends on the nature of the introduced azogroups. The introduction of the azo group – N=N – into the aromatic structure of tannin increases its thermal stability. On the contrary, the presence of a quaternary ammonium group makes the structure of tannin decrease its thermal stability. The main stages, kinetics, and proposed mechanism of pyrolysis during the period of intensive release of volatile substances were determined. Kinetic analysis was performed using both model-free and model-based methods. The results of the study indicate the inaccuracy of model-free methods, in contrast to model-based methods, in relation to the description of the kinetics of thermal decomposition of tannin. The model-based method of Coats-Redfern revealed that within the temperature range of 200-350 °C, the thermal decomposition of the initial tannin is constrained by a chemical reaction, likely of the second order (E = 118 kJ/mol). The thermal decomposition of the ATN sample at the second stage of thermolysis (260-340 °C) also takes place under conditions of a chemical reaction, most likely of the first order (E = 53 kJ/mol). For the CAT sample, it is challenging to select a decomposition model unambiguously within the temperature range of 280-340 °C. Models of chemical interaction, diffusion, and nucleus growth show similar high regression coefficients ($R^2 > 0.99$).

Keywords: tannins, azotannins, thermal decomposition, model-free and model-based methods, activation energy, mechanism of thermal decomposition

INTRODUCTION

Lignocellulosic biomass is a promising renewable source for the sustainable production of fuels and chemicals, which are currently produced mainly from fossil resources.[1-3] Plant-derived polyphenolic tannins are the fourth most abundant form of compounds extracted from terrestrial biomass, after cellulose, hemicelluloses, and lignin.[4] After lignin, tannins represent the most abundant source of natural aromatic macromolecules. Due to their renewable nature, low cost, and environmental safety, tannins can be potential substitutes for phenolic products, alternative feedstocks for chemical production, and building blocks for polymers and materials.[4-6]

Tannins can be divided into two categories: hydrolyzable and non-hydrolyzable or condensed tannins. Condensed tannins are the most common class of tannins and are oligomers and polymers composed of multiple flavonoid units. Typically, the condensation of tannin implies the presence of 3-8 flavonoid repeat units. Commercial condensed tannins are polyflavonoids most often extracted from the bark and wood of tropical acacia and mimosa plants or pine bark.[7] A suitable source of tannins can be larch bark, a characteristic feature of the chemical composition of the bark is the high content of polyphenolic compounds, represented mainly by lignin and condensed tannins (also

called proanthocyanidins), and the content of the latter reaches 12-15%.[8-10]

Condensed tannins have a higher reactivity compared to hydrolyzable tannins and therefore are of greater chemical and economic interest. Researchers are focused on studying the physical and chemical properties of organic polymers from condensed tannin due to the flexibility of its structure, high molar mass, reactivity and tendency of functionalization of the phenolic biopolymer. Due to the chemical composition of tannins, the presence of multiple aliphatic hydroxyls and phenolic hydroxyl groups, they are able to interact with a wide range of different compounds, including a number of organic compounds.

Nitrogen is currently the most used element in the scientific community for modifying the properties of tannins, and there are a variety of strategies developed for the introduction of nitrogen into organic polymers. Doping is used to change the chemical composition by adjusting the nature of the N-containing reagent, the initial pH, the amount of nitrogen precursor, *etc*.[11,12] Nitrogen-doped organic and carbon polymers obtained from tannins can be adapted for use as adsorbents, catalyst supports, materials for energy production and storage.[13] Over the past decades, the range of application of tannins as components of new materials of organic or carbon nature has significantly expanded, for example, in catalysis,[14] in the fields of ecology,[15,16] gas purification,[17] medicine[18] *etc.* At present, reactions such as amination[19] and azo coupling[20,21] are most often used to obtain N-modified tannins.

Recently, the use of azo coupling approaches allows obtaining N-containing biopolymers with a sufficiently high yield at room temperature, which is a valuable alternative production strategy. The advantages of the azo coupling reaction, including mild synthesis conditions, short reaction time and high yield, can provide a suitable configuration to meet the needs for the synthesis of polymers with azo bridges.

However, the widespread use of condensed tannins is limited by their insufficiently high solubility in water and some organic solvents. The simplest approach to increase polarity and, as a consequence, water solubility is, for example, cationization of tannins *via* phenolic functional groups by introducing quaternary ammonium groups. Cationization of polymers is considered an effective method to improve their performance for various applications and is a common practice, with 3-chloro-2-hydroxypropyltrimethylammonium chloride (CHPTAC) often used for this purpose.[22,23] Under strong acidity conditions, tannins can react with ethanolamines according to the Mannich reaction to give amphoteric tannins soluble in water.[24]

The functionalization of tannin with pH-sensitive and trans-cis-isomerization-sensitive light-induced diazobenzene groups not only increases its solubility in organic solvents and, in some cases, in water, but also opens up attractive possibilities for the creation of photosensitive materials.[25] The ability of tannins to protect against ultraviolet radiation is of interest for the creation of packaging materials.[26] Thus, the synthesis of modified nitrogen-annealed tannins isolated from larch bark is an interesting problem. In addition to providing numerous reactive hydroxyl groups, tannins can also impart good thermal stability. For example, tannin-based rigid foams have been reported to exhibit good thermal insulation properties.[27-29] This encourages further research to explore the possibilities and expand the applicability of tannin-based materials.

Unfortunately, compared to the pyrolysis of cellulose and lignin, there is limited information on the study of the pyrolysis of tannins. Some authors[30] investigated the pyrolysis of several model tannin compounds, including catechin and epicatechin, and indicated that catechol and 4-methylcatechol were the main pyrolysis products of the model compounds catechin and epicatechin. In another study,[31] the thermal decomposition of condensed tannins and their model compounds was studied using thermogravimetric analysis. The highest weight loss was observed at 197 °C for catechin, 159 °C for sulfited tannin, 189 °C for tannin acetate, and 271 °C for quebracho tannin (a commercial tannin extracted from quebracho).

Despite several similar studies, the question of the thermal nature of tannin transformations remains open. In this paper, we present a study of the thermal degradation of tannin and its N-derivatives. The study of the mechanism and kinetics of reactions involving solid compounds is a complex and difficult task, the complexity of which is due to a large number of factors with different effects, such as the rearrangement of the crystal lattice of a solid, the formation and growth of new crystallization nuclei, the diffusion of gaseous reagents or reaction products, the thermal conductivity of materials, *etc*.[32-34] Thermogravimetric (TG) methods are very useful because they provide reliable information on the physicochemical parameters characterizing the

processes of transformation of solids and their participation in isothermal or non-isothermal heating processes. For example, in previous research,[35] non-isothermal thermogravimetric analysis was used to study the thermal decomposition of sorghum straw, which occurred in three stages. The activation energy calculated using various isoconversional methods was 151 kJ/mol, 116 kJ/mol, and 137 kJ/mol for three pyrolysis zones, respectively. The kinetics and mechanism of pyrolysis of tannin-phenol-formaldehyde resins using isoconversional methods of analysis were studied in previous literature.[36] The average apparent activation energy of the pyrolysis stages was 109, 127, and 190 kJ/mol. Kinetic analysis is used for the mathematical description of the thermal decomposition process, which can be used to reproduce the original kinetic data, as well as to predict the kinetics of the process outside the experimental temperature range. The results obtained on this basis can be directly applied in materials science to obtain various synthetic or natural polymers and composite materials.

The purpose of this work is to study the process of thermal decomposition of the initial tannin and its N-modified products by TG/DTG analysis data, to find out kinetic data and the probable mechanisms of decomposition on the stage of intensive decomposition of tannin and its N-derivatives using model-free and model-based methods. The results of this study are expected to improve the understanding of the behavior of tannin and its N-modifiers during pyrolysis, to eliminate gaps in the literature on thermal decomposition kinetics, and improve the accuracy of kinetic models, bridging the gap between fundamental kinetics and industrial applications.

EXPERIMENTAL

Obtaining tannins (T)

Polyphenolic compounds were used as the starting material, the bulk of which was represented mainly by condensed pyrocatechol tannins, isolated by extraction of previously de-resined Siberian larch bark (*Larix sibirica* Ledeb), with a fraction of 3.5–2.2 mm, in an aqueous-ethanol solution. Tannins of the following composition (wt%) were used in the work: C – 59.7, H – 6.3, N – 0.9, O_{diff} – 33.1, ash – 0.3.

Preparation of azo derivatives of tannins by azo coupling of tannin with o-cyanophenyldiazonium chloride (azotannin nitrile (ATN))

0.83 g of anthranilic acid nitrile was dissolved in 14 mL of 5% hydrochloric acid solution. A solution of 0.56 g of sodium nitrite in 5 mL of water was added to the solution cooled to 0-5 °C with stirring, a few drops of 20% hydrochloric acid solution were added to dissolve the precipitate. The end of diazotization was determined using starch iodide paper. The solution was left in an ice bath for 30 min. 2 g of sodium acetate trihydrate in 7 mL of water was added to the diazonium salt solution, and then a solution of 1.2 g (0.007 mol per gallic acid) of tannin in 60 mL of 2% sodium hydroxide solution, cooled to 0 °C, was added under stirring. The resulting mixture was kept in the cold for 30 min. The mixture was evaporated in a vacuum to 1/3 of the volume and dialyzed on cellophane against distilled water for 10 hours. The solution in the dialysis bag was evaporated in a vacuum of a water-jet pump. The yield of the solid product was 0.80 g. The obtained compound has the following composition (% by weight): C – 54.0; H – 3.8; N – 9.8; O_{diff} – 32.4.

Cationization of larch tannin (cationic azotannin (CAT))

To a solution of 1.7 g tannin in 20 mL 2N aqueous NaOH solution was added 2 mL of 3-chloro-2-hydroxypropyl-trimethylammonium chloride (CHPTAC) under stirring at room temperature. The resulting mixture was heated to 70 °C and kept at this temperature for 3 hours. After the end of this time, the reaction mixture was cooled to room temperature, neutralized with ~20% H_2SO_4 to a neutral medium. It was evaporated in a vacuum of a water-jet pump to 1/3 of the volume, the residue was dialyzed on cellophane against distilled water for 24 hours, changing the water every hour. The contents of the dialysis bag were evaporated to dryness on a water-jet pump. The obtained compound had a yield of 0.95 g, and the following composition (% wt): C – 50.6; H – 7.2; N – 4.1; O_{diff} – 38.1.

Physicochemical research

FTIR spectra were recorded using a Tensor 27 FTIR spectrometer (Bruker, Germany). Spectral data were processed using the OPUS software (version 7.5). Solid samples for analysis were prepared as KBr pellets (5 mg sample/1000 mg KBr).

The elemental composition was studied using a Vario EL cube elemental analyzer (Elementar, Germany). Determination conditions: CHNS configuration, sample combustion in the presence of oxygen, followed by gas adsorption separation and detection of combustion products using a thermal conductivity detector.

The study of thermal decomposition of samples was carried out using the method of thermogravimetry/differential thermogravimetry (TG/DTG) in an argon atmosphere. Thermal analysis was performed in a corundum crucible using an STA 449 F1 Jupiter device (Netzsch, Germany) in the temperature range from 30 to 700 °C under argon flow (the flow rates of the protective and purging gases were

20 and 50 mL/min, respectively). The heating rate was 5, 10, and 20°/min. The measurement results were processed using the Netzsch Proteus Thermal Analysis 5.1.0 software package supplied with the device. The mass of the samples of the studied substances was 9 ± 0.01 mg.

RESULTS AND DISCUSSION

FTIR analysis

FTIR spectra of the original and modified tannins are shown in Figure 1. The FTIR spectra of both the original and modified tannins exhibit a broad absorption band at about 3400 cm^{-1}, which corresponds to the stretching absorption of hydroxyl groups found in both phenolic and aliphatic compounds. Additionally, the bands observed at approximately 2922, 2852 and 1366, 1447 cm^{-1} are assigned to the stretching and bending vibrations of C-H groups. The absorption band in the region of 1600-1700 cm^{-1} can be attributed to carbonyl groups conjugated with the aromatic ring structure. The presence of an aromatic skeletal structure in both the original and modified tannins is further supported by the absorption band corresponding to C-H vibrations of the aromatic ring, which appears at 1517 cm^{-1}.

The absorption band at 1282 cm^{-1} is attributed to phenyl-O stretching, and that at about 1200 cm^{-1} – to bending vibrations C-OH. Stretching C-O modes are mainly assigned to band at ~1108 and ~1067 cm^{-1} in the pyran ring of tannin. In contrast to the IR spectrum of the original tannin, the ATN spectrum exhibits a distinct absorption band at 2223 cm^{-1}, corresponding to the stretching vibrations of the C≡N bond.[37]

The FTIR spectrum of cationic tannin (CAT) reveals the absorption bands in the region of ~3030 cm^{-1}, which is attributed the stretching vibrations of C–H in the $–N^{+}(CH_3)_3$, the band of ~1481 cm^{-1} is related to asymmetric bending vibrations of C-H bonds of methyl groups attached to $N^{+}(CH_3)_3$. The peak with the maximum at 1095 cm^{-1} is a complex of bands (C–O phenols) attributed to stretching vibrations of the C–O–C ether bond (Ar–O–CH_2). The band at ~967 cm^{-1} is attributed to stretching vibrations of C-N^{+} bonds. This is evidence of the successful grafting of 3-chloro-2-hydroxypropyl-trimethylammonium chloride (3-chloro-2-hydroxypropyl-trimethylammonium chloride (CHPTAC)) into the tannin structure. This finding aligns consistently with those reported previously.[22]

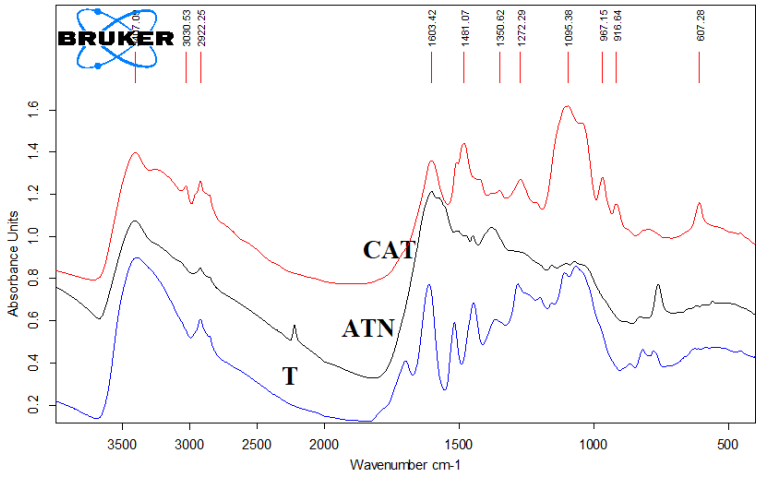

Figure 1: FTIR spectra of the initial tannin (T), azotannin nitrile (ATN) and cationic azotannin (CAT)

As a result of the tannin nitrogen combination reaction, significant changes in the fingerprint area occurred in the FTIR spectrum of the obtained azotannin nitrile (ATN) compared to the FTIR spectrum of the original tannin. The FTIR spectrum of the initial tannin contains a triplet of absorption bands in the range of 866-780 cm^{-1}, corresponding to non-planar deformation vibrations of the C-H bond with varying degrees of substitution of hydrogen atoms of the benzene ring. The FTIR spectrum of the ATN compound contains a doublet of absorption bands in the range of 825-760.5 cm^{-1} with an intense absorption band at 760.5 cm^{-1}. Since the production of cationic tannin is not associated with substitution reactions in the benzene ring, there are no significant changes in the FTIR spectrum of this derivative in

the fingerprint region, instead of three absorption bands, there is one wide band in this region.

A definitive assignment for the 607 cm^{-1} band is difficult. However, considering the nature of the molecule, it is most likely related to aromatic ring deformations or skeletal vibrations of the modified tannin structure.

TG Analysis

Figure 2 and Table 1 show the results of TG and DTG analyses of the initial and N-modified tannins. The TG and DTG curves can be divided into three main stages: (1) drying, (2) removal of volatiles and (3) formation of coke residue.

In the case of the initial tannin (T), sample drying ends at 133 °C. On the DTG curve (Fig. 2), this range corresponds to a distinct peak with a maximum rate of mass loss at 93 °C. The mass loss of the initial tannin when heated to 133 °C is 1.9% of the initial sample. The reason for this is probably the removal of surface water and light volatile compounds (CO_2, CO). The wide range of dehydration is associated with the difficulty of breaking hydrogen bonds between water molecules and polar functional groups of tannin, mainly hydroxyl ones. The second stage of thermolysis of T is associated with the decomposition of its main structure, which begins at 148 °C. These data are close to the onset temperature of decomposition of tannins from mimosa (146 °C),[38] pine (150 °C)[7] and tannins from pomegranate peel (149 °C).[39] The main decomposition of the initial tannin on the DTG curve is characterized by two peaks at 183 and 263 °C.

As reported previously,[30] pyrolysis of tannins primarily results in catechins, which exhibit a similar pattern during pyrolysis: two DTG peaks separated by an interval of 80 °C (230 and 310 °C). The shift in the interval of the main decomposition of the studied larch tannin towards lower temperatures can be explained by the presence of carbohydrates, which reduce the onset of thermal degradation.[31,40] The principal decomposition of T is completed at 308 °C. The mass loss in the second stage of thermal decomposition of tannin was 19.2%. Mass loss occurs due to the release of carbon dioxide upon heating (decarboxylation), the breaking of glycosidic bonds and the further loss of hydroxyls,[31] as well as the destruction of bonds in tannin molecules with the simultaneous formation of smaller phenolic compounds.[41,42]

The third stage of thermolysis of the original tannin sample is characterized by a lower intensity of volatile substances release and is probably associated with the polymerization of the tannin structure, forming a coke residue at the end of pyrolysis (46.1% of the initial sample). The mass loss in this stage was 32.4%. Significant structural changes occur in this stage, including the breakdown of aromatic rings and the further loss of hydroxyls.[41,42] Additionally, oxidation processes of the high-carbon residue (CO_2, H_2O, and CO) may occur, likely due to oxygen impurities in the argon purge gas or residual oxygen in the sample matrix. This aligns with prior research on biomass pyrolysis in an inert atmosphere.[43] In this stage, the remaining carbon-rich materials transform into charred material, a stable phase resistant to further degradation.

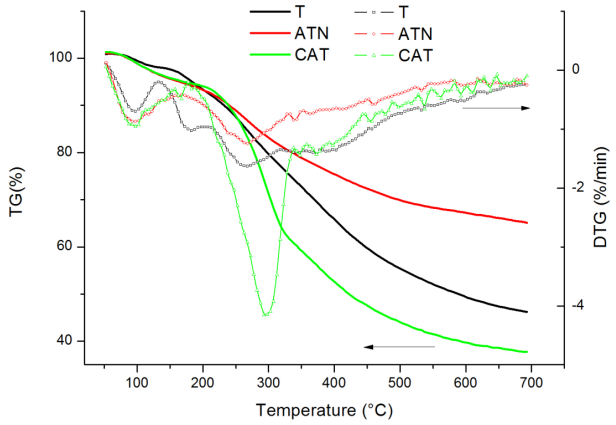

Figure 2: TG/DTG curves of original (T) and N-modified tannin samples (ATN and CAT) (heating rate 10 °C/min)

Table 1
TG/DTG data for samples of original tannin and its modified samples (heating rate 10 °C/min)

Sample	Stage	Onset temperature, T_0 (°C)	Peak temperature, T_{max} (°C)	Final temperature, T_f (°C)	Rate of mass loss (%/min)	Mass loss (%)	Residue at 700 °C (%)
T	I	30	93	133	0.69	1.9	46.1
	II	148	183 263	308	1.03 1.60	19.2	
	III	308	-	700	-	32.4	
ATN	I	30	98	168	0.87	5.0	64.9
	II	168	268	333	1.30	14.6	
	III	333	-	700	-	15.4	
CAT	I	30	98	178	0.96	5.2	37.5
	II	178	285	338	4.20	34.0	
	III	338	-	700	-	23.4	

The TG/DTG curves of ATN also show three apparent stages. Heating of the sample to 168 °C is characterized by the removal of adsorbed water, while the sample loses about 5% of its mass. On the DTG curve, this range corresponds to a peak with a maximum at 98 °C. The second stage characterizes the decomposition of the main structure of the ATN sample. The temperature range of the second stage is from 168 to 333 °C. The ATN sample started to decompose at 168 °C, which showed higher initial thermal stability than T. On the DTG curve, the second stage of thermolysis is marked by a wide peak with a temperature of the maximum in the mass-loss rate equal to 268 °C. In comparison with the initial tannin, the rate of mass loss in the second stage of ATN thermolysis decreased significantly. One can suppose that the azotannin molecule has a more stable structure, which raises the energy needed to break the bonds. This results in a lower decomposition rate. Additionally, a layer of decomposition products might form on the surface of the substance particle, shielding the inner layers of the material from further degradation. The mass loss in the second stage of thermolysis was 14.6%, which is less than in the case of T.

With further heating (the third stage), the sample continues to decompose, but with less intensity. The mass loss was 15.4%. At the end of pyrolysis, the residue was 64.9%, which is the maximum value for the samples studied in this study. The high value of the coke residue indicates high thermal stability of the substance. It can be assumed that the high thermal stability of the ATN sample is ensured by the presence of the azo group – N=N – in the aromatic structure,[44] contributing to the formation of a more stable framework that preserves structural integrity even under prolonged heating. A similar phenomenon is observed in studies of lignin nitrogen derivatives,[45] where it was found that the introduction of azogroups increases the overall stability of the material compared to the initial lignin.

The stage of water loss of the CAT sample has the widest temperature range among the studied samples (up to 178 °C). In this range, the sample loses 5.2% of the initial mass. On the DTG curve, this range corresponds to a peak with a maximum at 98 °C. It can be assumed that the high content of oxygen and hydrogen, according to the results of elemental analysis of the sample, suggests the presence of a greater number of hydroxyl and phenolic groups of different nature, which in turn ensures a high degree of dehydration in the initial stage of heating. During the second stage of thermolysis, the primary breakdown of the substance takes place, concluding at a temperature of 338 °C. This interval is characterized by an intense peak on the DTG curve, with a maximum at 285 °C. It is necessary to note the high rate of mass loss at the maximum point (4.2%/min), whereas for samples T and ATN this indicator, in the range of the main decomposition, was 1.6 and 1.3%/min, respectively. In addition, the CAT sample loses 34% of the initial sample during the second period, which is the maximum mass loss in the main stage of thermolysis among the studied samples. By analogy with the pyrolysis of cationic lignin,[23] the peak near 285 °C is probably associated with the thermal decomposition of the quaternary ammonium group. Accordingly, the cationic tannin has a lower thermal stability compared to the original, which can be explained by the elimination of quaternary ammonium groups from the cationic tannin. Similar results were published in the literature on the thermal

analysis of modified starch,[46,47] lignin,[48] hemicelluloses.[49] Some authors[50] showed that by treating cellulose with 3-chloro-2-hydroxypropyl-trimethylammonium chloride (CHPTAC), it was possible to significantly reduce the thermal stability of the biopolymer. During the heating process (stage 3) and up to the end of pyrolysis (700 °C), the intensity of mass loss significantly decreases. In this case, the sample loses 23.4% of its original mass. The coke residue at a temperature of 700 °C is 37.5%, which is the lowest among the studied compounds. It can be assumed that the quaternary ammonium group acts as an activator of thermal decomposition, accelerating the processes of depolymerization and decomposition. In addition, the introduction of additional polar centers causes the formation of new points of attack for thermal activation, increasing the likelihood of radical reactions.

Kinetic analysis

The apparent activation energy (E) can be accurately determined using model-free methods without the prior assumption of a reaction model, as recommended by the Kinetics Committee of the International Confederation for Thermal Analysis and Calorimetry (ICTAC Kinetics Committee).[51] In this study, the activation energies were calculated using the Ozawa-Flynn-Wall (OFW) and Friedman (F) methods.

The OFW method is an integral model-free method and is based on the following equation:[52]

$$\ln(\beta) = \ln\left(\frac{AE}{g(\alpha)\mathrm{R}}\right) - 5.3305 - 1.0516\frac{E}{RT} \qquad (1)$$

where β is the heating rate (K min^{-1}), A is the pre-exponential factor (s^{-1}), E is the apparent activation energy (kJ mol^{-1}), R is the gas constant (8.314 J mol^{-1} K^{-1}), T is the absolute temperature (K), and g(α) is an integral algebraic expression used to describe the mechanisms of solid-state processes.

The F method is an isoconversional or differential model-free method, which relates the logarithm of reaction rate with the inverse temperature for a constant α, based on the following equation:[53]

$$\ln\left(\frac{\mathrm{d}\alpha}{\mathrm{d}t}\right) = \ln\left[\beta\left(\frac{\mathrm{d}\alpha}{\mathrm{d}T}\right)\right] = \ln[Af(\alpha)] - \frac{E}{RT} \qquad (2)$$

where function $f(\alpha)$ is the differential form of the conversion-dependent function $g(\alpha)$.

The degree of conversion α was calculated using the formula:

$$\alpha = \frac{m_i - m_a}{m_i - m_f} \qquad (3)$$

where m_i is the initial mass of the sample; m_a is the actual mass; m_f is the mass at the end of thermal decomposition.

For a given α value, it is possible to estimate the values of E based on the slope of the lines obtained by plotting ln β versus 1/T (OFW) and $\ln\left(\frac{\mathrm{d}\alpha}{\mathrm{d}t}\right)$ versus 1/T (F), respectively.

Kinetic analysis of thermal decomposition was performed for the second stage of thermolysis of the samples, as the main volatilization processes take place in this stage.

It should be noted that the activation energy determined in this study is an apparent value, because in the case of complex reactions, the E parameter is a function of the activation energies of individual stages.

Figure 3 shows the dependence of the apparent activation energy on the degree of conversion of the second stage of thermal decomposition of T, ATN and CAT, based on the Ozawa-Flynn-Wall and Friedman methods.

In an ideal scenario, model-free analysis should provide consistent activation energies within the conversion range of 0.2 to 0.8, as per ICTAC guidelines.[54] Nevertheless, our findings (Fig. 3) revealed considerable variations in activation energy across this range, suggesting inaccuracies in model-free methods.

To evaluate the accuracy of the activation energy values, the Activation Energy Stability Index (SIE) was computed.[55] The index of activation energy stability was determined according to Equation (4):

$$\mathrm{SIE}\ (\%) = \frac{\max(E) - \min(E)}{\mathrm{mean}\ (E)} \times 100 \qquad (4)$$

A low SIE value (less than 15%) points to a single predominant reaction mechanism, whereas a high SIE (more than 25%) suggests multistep kinetics. The index was no lower than 36% for all the compounds examined. Therefore, it should be noted that within the studied temperature range, decomposition occurs through different mechanisms, and model-free methods cannot be used.

The use of model-based methods is due to a number of significant advantages over model-free methods in the context of the analysis of thermal decomposition of tannins. The thermal decomposition of complex compounds such as tannins often takes place in several stages, each of which follows its own patterns. Model-free methods are unable to take into account the complexity of the process, especially in the

presence of competing or interdependent reaction pathways.

Further, the kinetics of thermal decomposition was calculated using the model-based method of Coats-Redfern. This is a frequently method, first proposed in 1964.[56] Coats and Redfern, after making some approximations, proposed the following linear equation:

$$\ln\left(\frac{g(\alpha)}{T^2}\right) = \ln\left(\frac{AR}{\beta E}\right) - \frac{E}{RT} \quad (5)$$

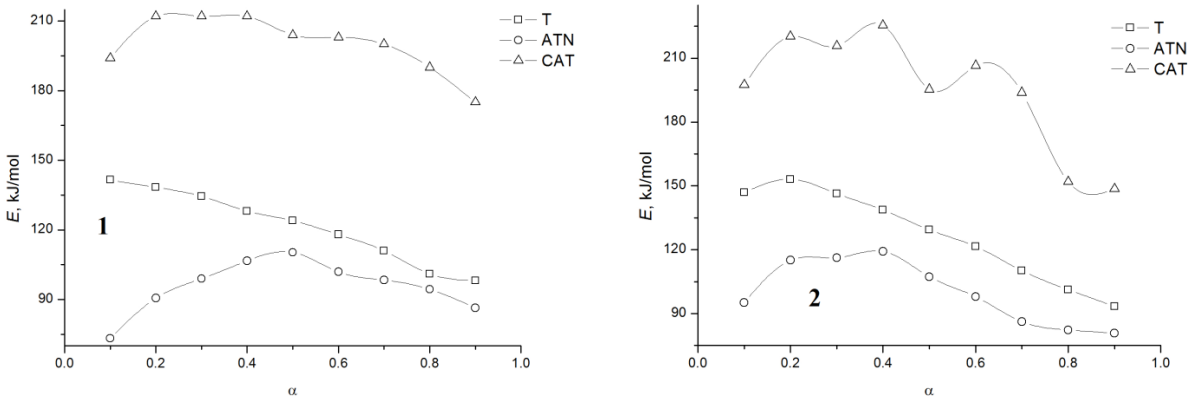

Figure 3: Apparent activation energy (E) distribution against the degree of conversion (α) of the second thermal degradation stage of the original tannin and its azo derivatives using Flynn-Wall-Ozawa (1) and Friedman (2) methods

Depending on the different decomposition processes, it is possible to obtain the value of E from the dependence of $\ln[g(\alpha)/T^2]$ versus $1/T$ using the $g(\alpha)$ indicated in Table 2. Then, the solution with the highest correlation coefficient (R^2) was chosen. Thus, it is also possible to obtain the most probable reaction mechanism.

Table 3 shows the results obtained for the studied substances at heating rates of 5, 10 and 20°/min. Table 3 shows that, in the temperature range of 200-350 °C, the thermal decomposition of the initial tannin is limited by a chemical reaction, most likely of the second order. The average value of the activation energy was 118 kJ/mol.

It can be assumed that decarboxylation occurs, a typical process observed when acid derivatives of phenols are heated. As a rule, this reaction begins at a temperature of about 200 °C and continues up to 350 °C. At high temperatures, the removal of CO_2 accelerates, which leads to the formation of low molecular weight carbonyl compounds. In addition, glycosidic bonds are destroyed and phenolic compounds are formed.

Table 2
Expressions of $g(\alpha)$ for kinetic model functions

Mechanism/Denotation	$g(\alpha)$
A geometric model of change in surface or volume	
Surface, *R2*	$1-(1-\alpha)^{1/2}$
Volume, *R3*	$1-(1-\alpha)^{1/3}$
Diffusion limitation	
One-dimensional diffusion, *D1*	α^2
Two-dimensional diffusion, *D2*	$(1-\alpha)\ln(1-\alpha)+\alpha$
Three-dimensional diffusion (Jander model), *D3*	$[1-(1-\alpha)^{1/3}]^2$
Three-dimensional diffusion (Ginstling-Brounstein model) *D*4	$1-2/3\alpha-(1-\alpha)^{2/3}$
Limiting reaction rate (reaction order)	
1st order reaction, *F*1	$-\ln(1-\alpha)$
2nd order reaction, *F*2	$[1/(1-\alpha)]-1$
3rd order reaction, *F*3	$½[(1-\alpha)^{-2}-1]$
Random nucleation and nuclei growth	
Two-dimensional, *A*2	$[-\ln(1-\alpha)]^{1/2}$
Three-dimensional, *A*3	$[-\ln(1-\alpha)]^{1/3}$

Table 3
Best fitted results of activation energy for the second thermal degradation stage for T, ATN and CAT

Substance	Heating rate 5°/min			Heating rate 10°/min			Heating rate 20°/min		
	Best model fit	*E* (kJ/mol)	R^2	Best model fit	*E* (kJ/mol)	R^2	Best model fit	*E* (kJ/mol)	R^2
T	F2	120.4	0.9758	F2	125.4	0.9761	F2	108.8	0.9759
	F1	85.2	0.9613	F3	152.4	0.9753	F1	76.6	0.9531
	A2	38.2	0.9516	F1	88.5	0.9617	F3	149.0	0.9489
ATN	F1	54.8	0.9737	F1	50.7	0.9845	F1	52.2	0.9734
	F2	76.3	0.9690	D3	100.6	0.9771	F2	79.1	0.9707
	D3	108.0	0.9651	A2	21.0	0.9755	D3	101.3	0.9617
CAT	F1	81.3	0.9964	F1	81.2	0.9944	F1	79.4	0.9957
	A2	36.4	0.9953	A2	36.3	0.9925	A2	35.2	0.9941
	D3	161.3	0.9944	D3	160.4	0.9905	D3	154.8	0.9913

In turn, the phenolic rings in the tannin structure are relatively resistant to low temperatures, but starting at about 200 ° C, there is a gradual breakdown of weaker intermolecular bonds, accompanied by the formation of small fragments of molecules containing phenolic nuclei. These fragments subsequently enter into further chemical transformations, forming degradation products.[31] Similar conclusions were repoted in the literature[56] for tannins isolated from *Acacia mollissima*.

The thermal decomposition of the ATN sample in the second stage of thermolysis (260-340 °C) also takes place under conditions of a chemical reaction, most likely of the 1st order. However, unlike the initial tannin, the average activation energy is reduced by almost half (53 kJ/mol). It is clear from the data of the elemental analysis that the H/C ratio of the ATN sample is minimal (0.07), whereas in the case of T and CAT, it is 0.11 and 0.14, respectively. As you know, this indicator characterizes the degree of aromaticity of a compound. The high degree of aromaticity of the compounds demonstrates a high thermal stability of the substance due to the structural features of the electronic shells and charge distribution. Consequently, despite the decrease in activation energy, the compound itself has a significant ability to maintain the integrity of its structure at elevated temperatures. Thus, fewer bonds are broken in this temperature range than in the original tannin.

Thermogravimetry results show that in the studied temperature range (260-340 °C), the mass loss of the sample was minimal. The observation of minimal mass loss in the temperature range under study further confirms our point of view. Despite the lowered energy barrier, the structure retains its integrity, which is manifested in the absence of a noticeable decrease in the weight of the sample. It can be assumed that the azo group (-N=N-) in the aromatic structure plays a key role in ensuring high thermal stability. The azo group forms a conjugated electronic system together with aromatic rings, increasing the overall stability of the molecule. Conjugated systems ensure uniform distribution of electron density, reducing local tension and protecting the structure from destruction. The -N=N- bonds in the azo group are characterized by high dissociation energy (~240 kJ/mol), which makes them difficult to convert under normal thermal conditions. This additional stability prevents the molecules from breaking down into individual fragments under moderate heat. During pyrolysis, stable structures are formed that can be maintained even under prolonged exposure to high temperatures. It is important to note that a decrease in the activation energy does not necessarily lead to an acceleration of destruction. In this case, the opposite effect is observed: although the activation barrier is lowered, the properties of the molecular structure itself make it more resistant to decomposition. In addition, the high content of coke residue is an indicator of the high thermal stability of the substance. This is due to the fact that the residue at the end of pyrolysis is a solid phase consisting mainly of carbonized residues of the starting material. If a significant proportion of the substance remains after thermal decomposition, it means that it had sufficient strength and resistance to high temperatures.

In the case of CAT, quaternary ammonium groups play an important role in stabilizing macromolecules, providing spatial separation of charged centers and preventing aggregation of molecules. When quaternary ammonium groups are removed, the steric resistance between the individual units of the macromolecule decreases,

making the compound vulnerable to damaging factors. Thus, the replacement of natural substituents with quaternary ammonium groups significantly reduces the thermal stability of the natural biopolymer.

For the second stage of CAT thermolysis, the models of chemical interaction, diffusion, and nuclear growth exhibit similar and high regression coefficients. The proximity of the regression coefficients for different models shows that each of the proposed models is equally successful in describing the observed data. The lack of significant differences in the quality of the approximation makes it difficult to unambiguously choose one of the models. Thermolysis in the specified temperature range (280-340 °C) is a complex multicomponent process involving several parallel reactions, each of which may have its own order and activation energy. Such a variety of possible mechanisms makes it difficult to identify the only correct option. According to the results of thermogravimetric analysis, the greatest mass loss is observed in the CAT sample. This fact is consistent with the assumption that active decomposition processes are taking place in the studied temperature range, leading to the release of large amounts of volatile substances. Given the difficulty of identifying a single leading mechanism, it is advisable to continue studying samples using additional diagnostic methods such as FTIR-spectroscopy and mass spectrometry combined with thermal analysis. Such additional analyses will allow for a deeper understanding of the nature of the changes taking place and identify specific decomposition products characteristic of each stage of thermolysis.

The obtained results on the thermal stability and kinetics of pyrolysis of azo derivatives of tannin are in good agreement with the broader context of research in the field of wood biomass processing. An integrated approach to the study of biopolymers of larch and other wood species allows not only for an in-depth investigation of their fundamental properties, but also for the development of effective methods for their modification to obtain valuable products. For example, studies on the hydrolysis of microcrystalline cellulose from birch wood on mixed oxide catalysts Al_2O_3-B_2O_3 demonstrate the potential for creating effective heterogeneous catalytic systems for the processing of polysaccharides.[57] In parallel, studies devoted to the isolation and subsequent sulfation of galactoglucomannan from larch wood open up ways of obtaining water-soluble derivatives of hemicelluloses with improved properties.[58] Furthermore, a detailed analysis of the molecular characteristics and antioxidant activity of spruce hemicelluloses obtained by catalytic oxidative delignification methods highlights the importance of a thorough understanding of the structure of natural polymers to predict their behavior under various conditions, including thermal exposure.[59] Thus, the study of the thermal degradation of N-modified tannins presented in this paper is an integral part of systematic efforts aimed at creating a scientific basis for the rational use of all components of lignocellulosic biomass.

CONCLUSION

The composition of the initial tannin isolated from larch and the obtained N-modified compounds based on it was analyzed by elemental analysis and FTIR spectroscopy. The results of FTIR spectroscopy confirm the formation of nitrile azotannin (ATN) and cationic azotannin (CAT) from the original tannin of larch. Unlike the original tannin, the FTIR spectrum of ATN contains an absorption band at 2223 cm^{-1}, corresponding to the stretching vibrations of the C≡N bond. The FTIR spectrum of cationic tannin (CAT) revealed absorption bands of quaternary ammonium in the region of 3030, 1481 and 967 cm^{-1}, which is evidence of grafting of 3-chloro-2-hydroxypropyl-trimethylammonium chloride (CHPTAC) to tannin.

The thermal degradation of larch tannin and its nitrided compounds was studied by thermogravimetric methods. The main stages of pyrolysis and the heat resistance of the studied substances were determined. It has been shown that the introduction of nitrile substituents into the structure increases, and the cationization of tannin by a quaternary ammonium group reduces the thermal stability of the compound.

Through careful kinetic analysis of the stage of the main release of volatile substances, it was established that model-free methods should not be used to study the structure of tannins. In turn, the use of model-based methods helped to determine the mechanism of thermal decomposition of the studied stage and to determine the values of the apparent activation energy. In particular, the nature of the thermal decomposition process of T and ATH is best represented in the context of specific kinetic models such as F2 and F1, respectively. The activation energy of the initial tannin in the second stage of thermolysis corresponded to 118 kJ/mol.

Despite the fact that the TGA results showed an increase in the thermal stability of the ATN sample, the values of the activation energy of decomposition occurring in the second stage of thermolysis were lower than the initial substance. The average activation energy is reduced by almost half (to 53 kJ/mol), which theoretically should contribute to an increase in the reaction rate. However, the terminological relationship between the activation energy and the reaction rate is not so simple. The activation energy describes the minimum energy threshold required to start a reaction, but does not uniquely determine its rate. The ATN sample showed a lower H/C ratio among the studied compounds, which characterizes the high aromaticity of this compound. A high degree of aromaticity is characterized by an increase in the resistance of molecules to external influences, such as an increase in temperature. The study showed that the introduction of the azo group into the structure of tannin increases its thermal stability. The obtained values show the significant potential of ATN for use in areas requiring high-temperature operation, such as fire-resistant coatings, insulating materials, and special-purpose composites.

Based on the TGA findings, the CAT sample exhibits lower thermal stability compared to T and ATN. This is indicated by the largest decrease in the mass of the sample in the second period of thermolysis, as well as the smallest residue at the end of pyrolysis. It is likely that the introduction of quaternary ammonium groups into the structure of tannin leads to a decrease in its thermal stability.

Kinetic analysis of the second stage of thermolysis of the CAT sample using the model-based method did not give an unambiguous conclusion about the prevailing mechanism of thermal decomposition. The models of chemical interaction (F), diffusion (D), and nuclear growth (A) show high similar regression coefficients ($R^2 >$ 0.99), which makes it difficult to choose the only optimal model. The temperature of the second stage of CAT thermolysis (280-340 °C) causes multiple competing reactions, each of which is characterized by its own mechanism and parameters. Such conditions make it difficult to accurately predict the behavior of the system, making it difficult to choose a specific model.

Future work will use TG-MS or TG-FTIR methods to identify volatile pyrolysis products (*e.g.* phenols, CO^2, and aldehydes) and elucidate decomposition pathways. *In situ* methods will provide a deeper understanding of the mechanisms.

The information obtained is useful for understanding the thermolysis processes of polymers and natural compounds containing tannins. It allows better planning the conditions for processing, synthesis and operation of materials, based on knowledge of the characteristics of individual components of the mixture.

ACKNOWLEDGEMENTS: This research was carried out within the budget plan FWES-2026-0010 for the Institute of Chemistry and Chemical Technology, Siberian Branch of the Russian Academy of Sciences, on the equipment of the Krasnoyarsk Regional Center for Collective Use, Krasnoyarsk Science Center.

REFERENCES

[1] K. David and A. J. Ragauskas, *Energ. Environ. Sci.*, **3**, 1182 (2010), https://doi.org/10.1039/B926617H

[2] P. Sannigrahi, A.J. Ragauskas and G. A. Tuskan, *Biofuels Bioprod. Biorefin.*, **4**, 209 (2010)

[3] A. Gasparatos, C. N. H. Doll, M. Esteban, A. Ahmed and T. A. Olang, *Renew Sustain Energy Rev.*, **70**, 161 (2017), https://doi.org/10.1016/j.rser.2016.08.030

[4] A.-K. Koopmann, C. Schuster, J. Torres-Rodríguez, S. Kain, H. Pertl-Obermeyer *et al.*, *Molecules*, **25**, 4910 (2020), https://doi.org/10.3390%2Fmolecules25214910

[5] A. Szczurek, V. Fierro, A. Pizzi, M. Stauber and A. Celzard, *Ind. Crop. Prod.*, **5**, 40 (2014), https://doi.org/10.1016/j.indcrop.2014.01.012

[6] N. M. Mikova, V. A. Levdanskiy, G. P. Skwortsova, A. M. Zhizhaev, M. A. Lutoshkin *et al.*, *Biomass Convers. Biorefin.*, **11**, 1565 (2021), https://doi.org/10.1007/s13399-019-00561-8

[7] C. Luo, W. Grigsby, N. Edmonds, A. Easteal and J. Al-Hakkak, *J. Appl. Polym. Sci.*, **117**, 352 (2010), https://doi.org/10.1002/app.31545

[8] N. M. Mikova, L. I. Grishechko, G. P. Skvortsova and B. N. Kuznetsov, *Chem. Plant Raw Mater.*, **4**, 41 (2017), https://doi.org/10.14258/jcprm.2017041840

[9] P. N. Diouf, C. M. Tibirna, M.-E. García-Pérez, M. Royer, P. Dubé *et al.*, *J. Biomater. Nanobiotechnol.*, **4**, 1 (2013), http://dx.doi.org/10.4236/jbnb.2013.43A001

[10] I. Miranda, J. Gominho, I. Mirra and H. Pereira, *Ind. Crop. Prod.*, **36**, 395 (2016), https://doi.org/10.1016/j.indcrop.2011.10.035

[11] F. Braghiroli, V. Fierro, A. Pizzi, K. Rode, W. Radke *et al.*, *Ind. Crop. Prod.*, **44**, 330 (2013), http://dx.doi.org/10.1016/j.indcrop.2012.11.024

[12] D. Salinas-Torres, A. F. Léonard, V. Stergiopoulos, Y. Busby, J.-J. Pireaux *et al.*, *Micropor. Mesopor. Mater.*, **256**, 190 (2018), https://doi.org/10.1016/j.micromeso.2017.08.004

[13] F. L. Braghiroli, V. Fierro, A. Szczurek, N. Stein, J. Parmentier *et al*., *Ind. Crop. Prod*., **70**, 332 (2015), https://doi.org/10.1016/j.indcrop.2015.03.046
[14] M. Gao, Z. Wang, C. Yang, J. Ning, Z. Zhou *et al*., *Colloids Surfaces A Physicochem. Eng. Asp*., **566**, 48 (2019), https://doi.org/10.1016/j.colsurfa.2019.01.016
[15] Q. Liu, Q. Liu, B. Liu, T. Hu, W. Liu *et al*., *J. Hazard. Mater*., **352**, 27 (2018), https://doi.org/10.1016/j.jhazmat.2018.02.040
[16] L. Huang, Q. Shuai and S. Hu, *J. Clean. Prod*., **215**, 280 (2019), https://doi.org/10.1016/j.jclepro.2019.01.040
[17] R. Bera, M. Ansari, A. Alam and N. Das, *J. CO_2 Utiliz*., **28**, 385 (2018), https://doi.org/10.1016/j.jcou.2018.10.016
[18] V. Uivarosi, A. C. Munteanu and A. Sharma, "Current Aspects of Flavonoids: Their Role in Cancer Treatment", Springer, Berlin, Germany, 2019
[19] K. Hashida, R. Makino and S. Ohara, *Holzforschung*, **63**, 319 (2009)
[20] J. X. Zhou, X. S. Luo, X. X. Liu, Y. Qiao, P. F. Wang *et al*., *J. Mater. Chem*., **6**, 5608 (2018), https://doi.org/10.1039/C8TA00341F
[21] G. Ji, Z. Yang, H. Zhang, Y. Zhao, B. Yu *et al*., *Angew. Chem. Int. Ed*., **55**, 9685 (2016), https://doi.org/10.1002/anie.201602667
[22] P. I. F. Pinto, S. Magina, E. Budjav, P. C. R. Pinto, F. Liebner *et al*., *Ind. Eng. Chem. Res*., **61**, 3503 (2022), https://doi.org/10.1021/acs.iecr.1c04899
[23] F. Kong, K. Parhiala, S. Wang and P. Fatehi, *Eur. Polym. J*., **67**, 335 (2015), https://doi.org/10.1016/j.eurpolymj.2015.04.004
[24] M. Zhang, J. Hou, Z. Yang, M. Wu, J. Wu *et al*., *Environ. Sci. Pollut. Res*., **30**, 34996 (2023), https://doi.org/10.1007/s11356-022-24583-4
[25] A. Duval, H. Lange, M. Lawoko and C. Crestini, *Biomacromolecules*, **16**, 2979 (2015), https://doi.org/10.1021/acs.biomac.5b00882
[26] Y. Zhai, J. Wang, H. Wang, T. Song, W. Hu *et al*., *Molecules*, **23**, 2073 (2018), https://doi.org/10.3390/molecules23082073
[27] G. Tondi, A. Pizzi and R. Olives, *Maderas Cienc. Technol*., **10**, 219 (2008), https://doi.org/10.4067/S0718-221X2008000300005
[28] C. Lacoste, M. C. Basso, A. Pizzi, M. P. Laborie, A. Celzard *et al*., *Ind. Crop. Prod*., **43**, 245 (2013), https://doi.org/10.1016/j.indcrop.2012.07.039
[29] N. M. Mikova, I. P. Ivanov, O. Yu. Fetisova, A. S. Kazachenko and B. N. Kuznetsov, *Bioresour. Technol. Rep*., **22**, 101454 (2023), https://doi.org/10.1016/j.biteb.2023.101454
[30] O. Seiji, Y. Yasuta and H. Ohi, *Holzforschung*, **57**, 145 (2003)
[31] M. Gaugler and W. J. Grigsby, *J. Wood Chem. Technol*., **29**, 305 (2009), https://doi.org/10.1080/02773810903165671
[32] L. Vlaev, N. Nedelchev, K. Gyurova and M. Zagorcheva, *J. Anal. Appl. Pyrol*., **81**, 253 (2008), https://doi.org/10.1016/j.jaap.2007.12.003
[33] S. C. Turmanova, S. D. Genieva, A. S. Dimitrova and L. T. Vlaev, *eXPRESS Polym. Lett*., **2**, 133 (2008), https://doi.org/10.3144/expresspolymlett.2008.18
[34] W. He, F. Deng, G.-X. Liao, W. Lin, Y.-Y. Jiang *et al*., *J. Therm. Anal. Calorim*., **100**, 1055 (2010), https://doi.org/10.1007/s10973-009-0515-4
[35] V. Dhyani, J. Kumar and T. Bhaskar, *Bioresour. Technol*., **245**, 1122 (2017), https://doi.org/10.1016/j.biortech.2017.08.189
[36] Z. Yi, C. Li, J. Jiang, J. Zhang, W. Zhang *et al*., *J. Therm. Anal. Calorim*., **121**, 867 (2015), https://doi.org/10.1007/s10973-015-4625-x.
[37] L. J. Bellamy, "The Infra-Red Spectra of Complex Molecules", London, Chapman and Hall, 1975, 433 p.
[38] H. Saad, A. Khoukh, N. Ayed, B. Charrier and F. C.-E. Bouhtoury, *Ind. Crop. Prod*., **61**, 517 (2014), https://doi.org/10.1016/j.indcrop.2014.07.035
[39] O. V. Kharissova, L. M. Torres-Martínez and B. I. Kharisov, "Handbook of Nanomaterials and Nanocomposites for Energy and Environmental Applications", Springer, Cham, 2021, https://doi.org/10.1007/978-3-030-36268-3_182
[40] S. Ben Mahmoud, H. Saad, B. Charrier, A. Pizzi, K. Rode *et al*., *Wood Sci. Technol*., **49**, 205 (2015), https://doi.org/10.1007/s00226-014-0686-4
[41] Z. Sebestyén, E. Jakab, E. Badea, E. Barta-Rajnai, C. Şendrea *et al*., *J. Anal. Appl. Pyrol*., **138**, 178 (2019), https://doi.org/10.1016/j.jaap.2018.12.022
[42] M. A. Pantoja-Castro and H. González-Rodríguez, *Rev. Latinoam. Quim*., **39/3**, 107 (2011)
[43] M. A. Islam, H. Bao, B. B. Saha and T. Takai, *Therm. Sci. Eng. Prog*., **56**, 103075 (2024), https://doi.org/10.1016/j.tsep.2024.103075
[44] G. Simeonov, A. Draganov and D. Ructschev, *J. Therm. Anal. Calorim*., **41**, 201 (1994), https://doi.org/10.1007/BF02547025
[45] V. S. Borovkova, Y. N. Malyar, N. Yu. Vasilieva, A. M. Skripnikov, V. A. Ionin *et al*., *Materials*, **16**, 1525 (2023), https://doi.org/10.3390/ma16041525
[46] Y. B. Wang and W. L. Xie, *Carbohyd. Polym*., **80**, 1172 (2010), https://doi.org/10.1016/j.carbpol.2010.01.042
[47] N. K. Goel, M. S. Rao, V. Kumar, Y. K. Bhardwaj, C. V. Chaudhari *et al*., *Radiat. Phys. Chem*., **78**, 399 (2009)
[48] C. Moore, W. Gao and P. Fatehi, *Polymers*, **13**, 3871 (2021), doi.org/10.3390/polym13223871
[49] J. L. Ren, R. C. Sun, C. F. Liu, L. Lin and B. H. He, *Carbohyd. Polym*., **67**, 347 (2007), https:/doi.org/10.1016/j.carbpol.2006.06.002
[50] G. Li, Y. Fu, Z. Shao, F. Zhang and M. Qin, *BioResources*, **10**, 7782 (2015)
[51] S. Vyazovkin, A. K. Burnham, J. M. Criado, L. A. Perez-Macheda, C. Popescu *et al*., *Thermochim. Acta*, **520**, 1 (2011), https://doi.org/10.1016/j.tca.2011.03.034
[52] T. A. Ozawa, *Bull. Chem. Soc. Jpn*., **707**, 1881 (1965)
[53] H. L. Friedman, *J. Polym. Sci. Part C Polym. Symp*., **6**, 183 (1964)

[54] S. Vyazovkin, A. K. Burnham, L. Favergeon, N. Koga, E. Moukhina *et al*., *Thermochim*. *Acta*, **689**, 178597 (2020), https://doi.org/10.1016/j.tca.2020.178597
[55] M. Marouani, L. Hamdaoui, Z. H. Alhalafi, A. Bellaouchou and L. Trif, *Biomass Bioenerg*., **202**, 108228 (2025), https://doi.org/10.1016/j.biombioe.2025.108228
[56] A. W. Coats and J. P. Redfern, *Nature*, **201**, 68 (1964), https://doi.org/10.1038/201068a0
[57] N. Tarabanko, S. V. Baryshnikov, A. S. Kazachenko, A. V. Miroshnikova, A. M. Skripnikov *et al*., *Wood Sci*. *Technol*., **56**, 437 (2022), https://doi.org/10.1007/s00226-022-01363-4
[58] A. S. Kazachenko, Y. N. Malyar, N. Vasilyeva, O. Y. Fetisova, A. I. Chudina *et al*., *Wood Sci*. *Technol*., **55**, 1091 (2021), https://doi.org/10.1007/s00226-021-01299-1
[59] V. S. Borovkova, Y. N. Malyar, I. G. Sudakova, A. I. Chudina, A. M. Skripnikov *et al*., *Molecules*, **27**, 266 (2022), https://doi.org/10.3390/molecules27010266